EFFECT OF STARCH ACCUMULATION IN HUANGLONGBING SYMPTOMATIC LEAVES ON REFLECTING POLARIZED LIGHT

Alireza Pourreza, Won Suk Lee

Department of Agricultural and Biological Engineering
University of Florida
Gainesville, Florida

ABSTRACT

Huanglongbing (HLB) or citrus greening disease is an extremely dangerous infection which has severely influenced the citrus industry in Florida. It was also recently found in California and Texas. There is no effective cure for this disease reported yet. The infected trees should be identified and removed immediately to prevent the disease from being spread to other trees. The visual leaf symptoms of this disease are green islands, yellow veins, or vein corking; however, starch accumulates on infected leaf and causes some blotchy mottle which is the finest diagnostic leaf symptom. Still it is not easy to decide the blotchy mottle is the results of starch accumulation or nutrient deficiency. Starch can rotate the polarization planar of light at a specific waveband. In this study, a vision sensor was developed based on this property of starch to detect the blotchy mottle on HLB infected citrus leaf and differentiate it from similar symptoms caused by nutrient deficiencies. A highly sensitive monochrome camera and 10 high power narrow band LEDs at 591 nm were used in this sensor. Also a polarizing film and a polarizing filter were mounted in perpendicular directions in front of the LED panel and the camera lens correspondingly. Therefore, the camera receives the minimum reflection. Since starch rotates the polarization planar of light, the sensor is able to highlight the accumulation of starch on the leaf. The narrow band polarized illumination condition was compared to non-polarized natural white light for leaf samples in healthy, HLB symptomatic, and nutrient (zinc) deficient conditions. The result showed that the developed vision sensor increasingly highlighted the HLB symptomatic areas on the leaf which contained more starch. Additionally, the separability among four different citrus leaf classes were compared before and after being ground, to investigate if the starch in ground infected leaves can be identified as good as unground leaves. The results showed that the freeze-dried ground leaves had more uniform brightness; but the starch accumulation could be identified more clearly.

Keywords: Citrus Disease, Huanglongbing, Image analysis, Starch, Vision Sensor.

INTRODUCTION

Citrus greening disease which is also called Huanglongbing (HLB) is an extremely destructive psyllid-spread infection in citrus. The insect can carry the bacteria and transfer it to healthy trees when they feed leaves. It was first seen in south Florida in 2005; however, today it can be seen in the entire state of Florida as well as some parts of California and Texas. Bitter taste, uneven shape, and irregular color are some indications of the HLB disease. But one of the visible symptoms of HLB is yellowish islands on the leaf which is due to the accumulation of starch. Although this symptom can be used for human-based infection identification, it would be very inaccurate most of the time because some nutrient deficiencies (such as zinc and magnesium deficiencies) generate similar symptom. Although, no effective treatment has been reported for HLB disease yet, an early diagnosis and elimination of the HLB affected trees can prevent more spread of the infection and avoid a huge loss.

Several HLB diagnostic approaches have been examined and introduced by researchers. These approaches can be categorized by human inspection (Futch et al., 2009), laboratory based starch measurement (Gonzalez et al., 2012), laboratory based qrt-PCR test (Hansen et al., 2008), airborne imaging (Li et al., 2011), and vision/spectroscopy based (Mishra et al., 2007; Pourreza et al., 2013) methods. Etxeberria et al. (2009) showed that an HLB affected citrus leaf includes an excessive amount of starch accumulation. They introduced a laboratory based starch measurement method to diagnose the symptomatic areas on the leaf and confirm if the symptoms were due to HLB disease or nutrient deficiency. However, their method required sample collection and laboratory works which was time consuming and labor intensive.

Kim et al. (2009) analyzed color microscopic images to identify the HLB infection on citrus leaf. They achieved an overall accuracy of 87% in HLB diagnosis using textural features extracted from the citrus leaf images.

Researchers showed that spectroscopy of ground citrus leaves can reveal the HLB status of samples. Hawkins et al. (2010) achieved the accuracy of over 95% in recognizing HLB affected leaves from healthy samples by analyzing the reflectance data of ground leaves in the mid-infrared band. Sankaran et al. (2010) employed a mid-infrared spectroscopy to classify ground leaves into HLB positive, HLB negative, or nutrient deficient classes and they obtained the accuracy of over 90% in HLB identification. In another study (Windham et al., 2011), the reflectance of ground leaves were used to identify HLB affected samples from healthy, nutrient deficient, and also other citrus disease. They obtained true positive rates of over 92% for different classes.

In our previous study (Pourreza et al., 2014), it was shown that the excessive starch level on HLB affected citrus leaves can be highlighted using the proposed image acquisition system. Later another vision sensor was developed which improved the efficiency of the original prototype. Therefore, the main objective of this study was to evaluate the performance of the proposed vision sensor and to confirm its efficiency. The specific goals were: (1) to assess the improvement in HLB identification achieved using the narrow band illumination and polarizing filters in comparison with a natural imaging condition, and (2) to compare the

effect of starch accumulation on the images of citrus leaves and ground leaf samples.

MATERIALS AND METHODS

Data Collection

Two datasets of Hamlin sweet orange leaves were collected from citrus trees in the Citrus Research and Education Center (CREC), University of Florida (Lake Alfred, Florida). The first dataset included 60 samples of HLB-negative, HLB-positive and zinc-deficient leaves which were used to compare the images acquired by the proposed vision sensor with those of the same samples obtained with a regular digital color camera. The second dataset included another 30 samples of HLB-negative, HLB-positive and Zinc-deficient leaves which was employed to compare the citrus leaf images before and after being ground. A qrt-PCR examination (Hansen et al., 2008) was performed on all the 90 samples in both datasets to confirm the HLB status of the leaves. The qrt-PCR test was conducted in the U.S. Sugar Corporation's Southern Gardens processing plant (Clewiston, FL).

Image acquisition

According to the results of the previous study (Pourreza et al., 2014), the accumulated starch in an HLB infected leaf causes a rotation in the light's polarization mainly around 600 nm. This capability was employed to develop a vision based sensor which was able to highlight the HLB symptomatic areas on an affected leaf with excessive amount of starch. The vision sensor included a monochrome camera (DMK 23G445, TheImagingSource, Bremen, Germany) with high sensitivity at 591 nm, and 10 high power (10 W) narrow band LEDs (LZ4-00A100, LED Engin, San Jose, California) concentrated at 591 nm (Fig. 1a) which were mounted in a 13 × 19 × 15 cm wooden box (Fig. 1b). Five LED drivers (RCD-48, RECOM, Brooklyn, New York) were used to power the LEDs as shown in Fig. 1c. A wide lens with 6 mm focal length was used for the camera to maximize its depth of field. Also one linear polarizer was installed in front of the camera's lens and another polarizing film (visible linear polarizing laminated film, Edmund Optics, Barrington, New Jersey) with a perpendicular direction to the camera filter was fixed in front of LED panel (Fig. 1b). Using this setting, the camera only receives the minimum reflection.

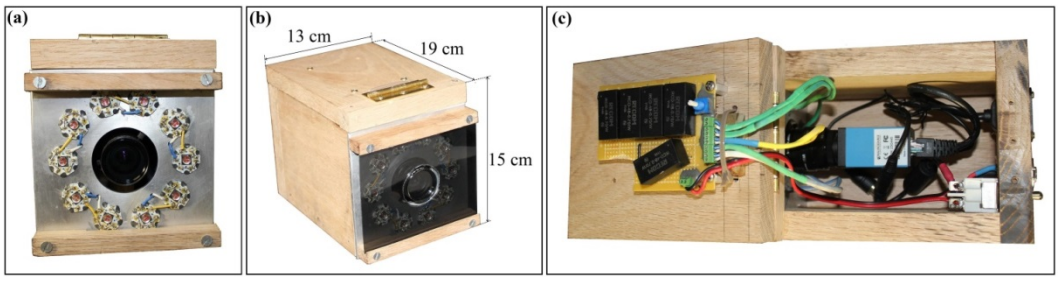

Fig. 1. Image acquisition system: (a) the box dimensions, (b) a front view of the LEDs panel, and (c) LED drivers and the camera inside the box.

Discriminant analysis

In order to compare the separability between the classes, Fisher ratio was used as the separability index and it was calculated using the features extracted from the images. Fisher ratio is defined as a ratio of the between-class variability to the within-class difference (Han et al., 2013). Equation 1 shows the Fisher ratio for one feature in a 2-class problem.

$$F_{ij} = \frac{(\mu_i - \mu_j)^2}{(\sigma_i^2 + \sigma_j^2)} \quad (1)$$

Where μ_i and μ_j are the means and σ_i and σ_j are the standard deviations in class i and j and F_{ij} shows the degree of the class separability in the direction of the corresponding feature. However, two features (gray values' mean and standard deviation) were employed in this experiment and the effect of both of them on a single separability index was needed. Therefore, a Fisher's linear discriminant analysis (LDA) was used to reduce the dimensions of feature vector to one for each pair of classes (Bishop, 2006). Then the Fisher ratio was calculated for the corresponding pair of classes. In Fisher's LDA, a function is employed to project the vector x down to one dimension (equation 2).

$$y = w^T x \quad (2)$$

The projection method in the Fisher's LDA was employed because it optimizes the weight vector (w) by maximizing the separation between the projected classes and minimizing variation within each projected class (equation 3).

$$w \propto S_W^{-1}(\boldsymbol{m}_2 - \boldsymbol{m}_1) \quad (3)$$

Where S_W is the total within class covariance matrix, and $\boldsymbol{m}_1$ and $\boldsymbol{m}_2$ are the mean of class one and two correspondingly. Using this projection, the Fisher ratio was computed between each pair of classes; however, there were four classes and consequently a separability index considering all four classes was needed. For this purpose, an arithmetic average of Fisher ratios for all possible pairs of classes was computed (equation 4) and considered as the general separability index (F) for comparison of HLB identification efficiencies between sensor images and RGB images.

$$F = \frac{\sum_i^C \sum_j^C P_i P_j F_{ij}}{C(C-1) \sum_i^C \sum_j^C P_i P_j} \quad (4)$$

Where P_i and P_j are proportional to the number of samples in classes i and j, and C indicates the number of classes.

Imaging conditions evaluation

The images of the citrus leaf samples in the first dataset were acquired in a completely dark room with the vision sensor from a distance of 80 cm. Therefore, the leaf samples only received the narrow band polarized light produced by the sensor. In order to evaluate the HLB identification efficiency of the sensor, another set of images from the same dataset were created using a regular color (RGB) digital camera (EOS Rebel T2i, Canon, Tokyo, Japan) and common indoor fluorescent light. All the RGB images were captured with a manual mode using shutter speed of 0.04 s, focal ratio of F4.5, and sensitivity of ISO800 to confirm the imaging condition uniformity and prevent the effect of camera settings on the

evaluation results. The histograms of the red, green, blue, and gray (average of red, green, and blue) components of the RGB color space and relative luminance (Y), blue-difference (Cb), and red-difference (Cr) components of the YCbCr color space were extracted from the symptomatic areas on each leaf and compared with the same symptomatic areas on the images captured by the vision sensor. Also the mean and standard deviation features of the leaf area were extracted from the vision sensor images and seven color components of the color images to evaluate the separability among the four classes of HLB-positive, zinc-deficient HLB-positive, zinc-deficient HLB-negative, and HLB-negative leaves.

Samples conditions evaluation

The leaf images in the second sample set were compared with the same samples after being ground; to investigate if the starch in ground infected leaves can be identified as good as unground leaves. For grinding process, first the samples were placed in a ceramic mortar and freeze-dried with liquid nitrogen (Sankaran et al., 2010) and then they were ground using a ceramic pestle. The gray values' means and standard deviations were extracted from both leaves and ground leaf images to evaluate the separability indexes (Fisher ratio) as explained in the previous section.

RESULTS

Dataset Validation

The number of required cycles for the fluorescent intensity to reach the threshold is considered as the cycle threshold (CT) in a qrt-PCR test. Li et al. (2006) suggested the CT value threshold of 33 to decide the HLB status of a sample. According to their study, a CT value smaller than 33 indicates the HLB-positive status, while a CT value over 33 does not show any HLB infection for the corresponding sample.

The first dataset included 20 zinc-deficient and 40 non-zinc-deficient samples. Based on the qrt-PCR test results 20 out of 40 non-zinc-deficient samples were HLB-positive and the other 20 samples were HLB-negative. Within the zinc-deficient class, 10 samples had the CT values below 33 and the rest of samples in this class had the CT values over 33. Therefore, the zinc-deficient class was divided into two subclasses of zinc-deficient HLB-positive (10 samples) and zinc-deficient HLB-negative (10 samples) classes.

The second dataset contained 10 HLB-positive, 10 HLB-negative samples in the non-zinc-deficient superclass. Seven samples within the zinc-deficient class had the CT values smaller than 33 and three zinc-deficient samples had the CT values bigger than 33. So they were subcategorized in zinc-deficient HLB-positive and zinc-deficient HLB-negative classes, correspondingly.

Comparison of imaging conditions

The arithmetic averages of separability indexes of 0.528, 0.201, 0.196, 0.136, 0.135, 0.134, 0.114, and 0.003 were achieved for the vision sensor, Cb component (YCbCr), Cr component (YCbCr), green component (RGB), Y component (YCbCr), gray component (RGB), red component (RGB), and blue component (RGB) respectively. Figure 2 shows the pairwise Fisher ratios for top three images including the vision sensor (green columns) and two components of color images (blue and purple columns). The Fisher ratios for vision sensor images were much bigger than the other two color components for all pairs of classes except for the HLB-negative/HLB-positive and HLB-negative/zinc-deficient HLB-positive pairs in which the ratios were quite similar. The minimum separability index (0.286) was achieved for the pair of HLB-positive/zinc-deficient HLB-negative (Cr component) and the maximum separability index (27.94) was obtained for the pair HLB-negative/zinc-deficient HLB-negative in vision sensor images.

Comparison of samples conditions

Figure 3 shows the pairwise Fisher ratios for samples in the second dataset before and after being ground. The arithmetic averages of separability indexes of 0.415, and 0.559 were obtained for the samples before and after grinding correspondingly. The Fisher ratios did not change a lot after grinding for all samples except for the HLB-negative/zinc-deficient HLB-negative pair in which the separability index increased extremely after grinding. The minimum separability index (0.097) belonged to the pair of HLB-positive/zinc-deficient HLB-positive after grinding.

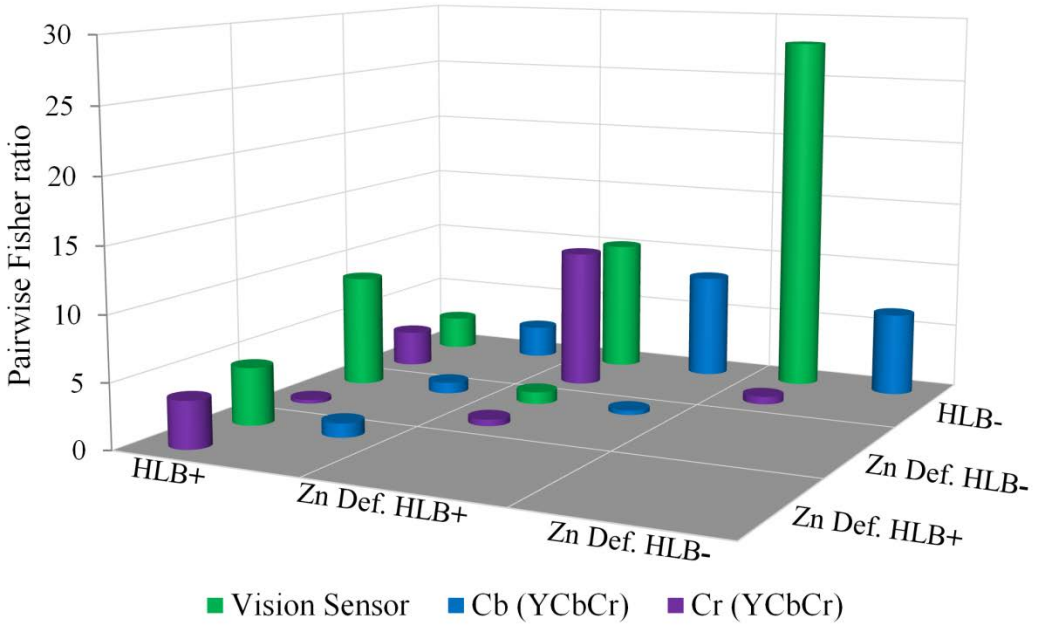

Fig. 2. Comparison of the pairwise Fisher ratios between the top three images: Vision sensor and Cb and Cr components of the YCbCr color space.

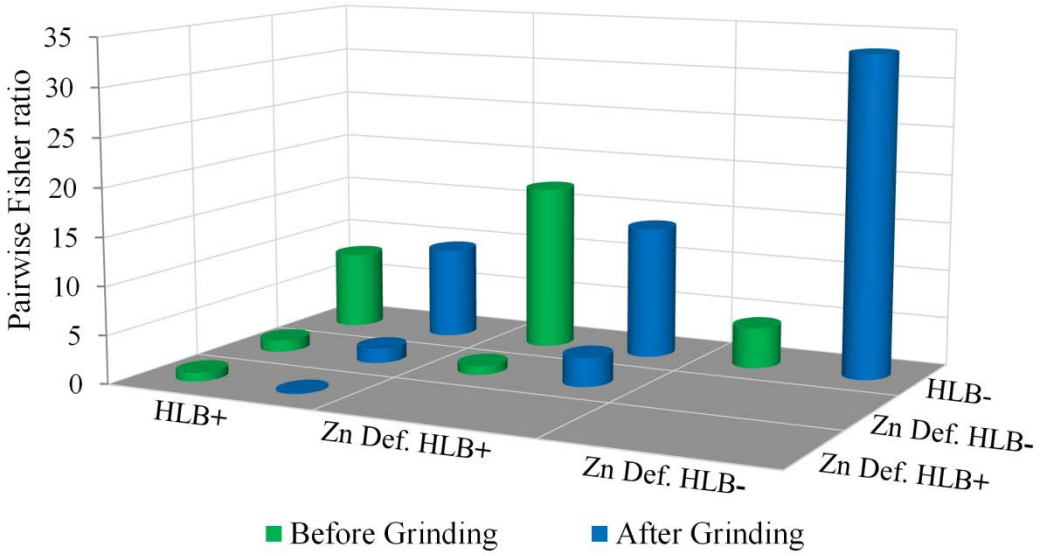

Fig. 3. Comparison of the pairwise Fisher ratios between samples before and after grinding.

DISCUSSION

The purpose of this study was to assess the HLB diagnosis efficiency of the proposed vision sensor. Two experiments were designed for this purpose in which the performance of the proposed method was compared with other methods. The dataset in each experiment contained four classes of citrus leaves including HLB-positive, HLB-negative, zinc-deficient HLB-positive, and zinc-deficient HLB-negative samples. Two image descriptors, gray values' mean and standard deviation, were extracted from each sample image and were used for data analysis. A separability index was introduced in this paper to numerically indicate how good the classes were distinguishable.

The vision sensor which was developed for the HLB diagnosis purpose was able to acquire the minimum reflection of a sample at 591 nm. In the first experiment, the images acquired by the vision sensor were compared to the color images of the same samples taken by a commercial color camera. Seven color components were extracted from the color images and the separability indexes were calculated for six possible pairs of classes individually. Then the arithmetic average of all six separability indexes was used to indicate the overall separability. The results confirmed an improved separability between the four classes in the vision sensor images compared to the color components. The HLB-positive/zinc-deficient HLB-negative and HLB-negative/zinc-deficient HLB-negative pairs of classes were more separable in the vision sensor images (figure 2). However, the separability indexes for HLB-positive/HLB-negative, and zinc-deficient HLB-positive/zinc-deficient HLB-negative pairs were fairly similar in the vision sensor images and Cb and Cr components. Generally, the HLB-positive/HLB-negative separability decreased within the zinc-deficient superclass because zinc deficiency generates some symptoms similar to HLB infection symptoms. It can be concluded that the HLB diagnosis is more difficult for zinc-deficient citrus leaves.

In the second experiment, the citrus leaf images acquired by the vision sensor were compared before and after being ground to determine if the starch accumulation is more detectable for ground leaves. Generally citrus leaves were brighter after being ground with a more uniform brightness. Back sides of a citrus leaf was brighter than its front side and after grinding, both sides of the leaves were mixed and could be seen by the sensor. That might be the reason of brighter gray values in the ground leaf images. The arithmetic average of Fisher ratio (separability index) increased slightly after grinding. The separability indexes between HLB-positive/HLB-negative classes increased within both zinc-deficient and non-zinc-deficient samples. It can be inferred that the starch accumulation was better detectable in the ground leaves, even though it was well highlighted in the unground leaves.

This vision sensor can be mounted on a tractor or an unmanned aerial vehicle (UAV) along with a differential Global Positioning System (DGPS) to conduct an automatic on-the-go diagnosis and create a map of HLB disease distribution in the grove.

CONCLUSION

In this study, a vision sensor was introduced for HLB disease diagnosis and its performance was assessed in two experiments. A customized illumination system along with two polarizing filters were designed for the vision sensor to enable it highlight the HLB infection symptoms on the citrus leaf and differentiate them from nutrient deficiency symptoms. The results showed that the recommended illumination at 591 nm and proper use of polarizing filters improved identification of the HLB symptom (starch accumulation). Further it was illustrated that the starch accumulation in the ground citrus leaves were better detectable compared to unground leaves; however, the separability indexes achieved form analyzing the unground leaf images were good enough for an on-the-go HLB diagnosis system. A set of inexpensive components were used to assemble the proposed vision sensor and it can be reproduced with less than a thousand dollars. Therefore, it can be a very worthy investment especially for small growers to conduct a constant HLB disease monitoring in their grove and prevent a huge loss in the future.

ACKNOLEGEMENT

This project was funded by the Citrus Research and Development Foundation, Inc. The authors would like to thank Drs. Reza Ehsani, Edgardo Etxeberria, Arunava Banerjee, and Ms. Veronica Campbell at the University of Florida and Mr. Michael Irey in the United States Sugar Corporation, Clewiston, FL for their assistance in this study.

REFERENCES

Bishop, C. M. 2006. *Pattern recognition and machine learning*. 1st ed., New York: Springer Science.

Etxeberria, E., P. Gonzalez, D. Achor, and G. Albrigo. 2009. Anatomical distribution of abnormally high levels of starch in HLB-affected Valencia orange trees. *Physiological and Molecular Plant Pathology* 74(1): 76-83.
Futch, S., S. Weingarten, and M. Irey. 2009. Determining HLB infection levels using multiple survey methods in Florida citrus. *Proceedings Florida State Horticultural Society (FSHS)* 122: 152-158.
Gonzalez, P., J. Reyes-De-Corcuera, and E. Etxeberria. 2012. Characterization of leaf starch from HLB-affected and unaffected-girdled citrus trees. *Physiological and Molecular Plant Pathology* 79: 71-78.
Han, J.-S., S. W. Lee, and Z. Bien. 2013. Feature subset selection using separability index matrix. *Information Sciences* 223(0): 102-118.
Hansen, A., J. Trumble, R. Stouthamer, and T. Paine. 2008. A new huanglongbing species,"Candidatus Liberibacter psyllaurous," found to infect tomato and potato, is vectored by the psyllid Bactericera cockerelli (Sulc). *Applied and Environmental Microbiology* 74(18): 5862-5865.
Hawkins, S. A., B. Park, G. H. Poole, T. Gottwald, W. R. Windham, and K. C. Lawrence. 2010. Detection of citrus huanglongbing by Fourier transform infrared–attenuated total reflection spectroscopy. *Applied spectroscopy* 64(1): 100-103.
Kim, D. G., T. F. Burks, A. W. Schumann, M. Zekri, X. Zhao, and Q. Jianwei. 2009. Detection of Citrus Greening Using Microscopic Imaging. *Agricultural Engineering International: the CIGR Ejournal*.
Li, W., J. S. Hartung, and L. Levy. 2006. Quantitative real-time PCR for detection and identification of Candidatus Liberibacter species associated with citrus huanglongbing. *Journal of Microbiological Methods* 66(1): 104-115.
Li, X., W. S. Lee, M. Li, R. Ehsani, A. R. Mishra, C. Yang, and R. L. Mangan. 2011. Comparison of different detection methods for citrus greening disease based on airborne multispectral and hyperspectral imagery. Paper No. 1110570. Louisville, Kentucky: ASABE.
Mishra, A., R. Ehsani, G. Albrigo, and W. S. Lee. 2007. Spectral Characteristics of Citrus Greening (Huanglongbing). ASABE Paper No. 073056. Minneapolis, Minnesota: ASABE.
Pourreza, A., W. S. Lee, E. Raveh, R. Ehsani, and E. Etxeberria. 2014. Citrus Huanglongbing Disease Detection Using Narrow Band Imaging and Polarized Illumination. *Trans. ASABE* 57(1): 259-272.
Pourreza, A., W. S. Lee, E. Raveh, Y. Hong, and H.-J. Kim. 2013. Identification of citrus greening disease using a visible band image analysis. Paper No.: 131591910. Kansas City, Missouri: ASABE.
Sankaran, S., R. Ehsani, and E. Etxeberria. 2010. Mid-infrared spectroscopy for detection of Huanglongbing (greening) in citrus leaves. *Talanta* 83: 574-581.
Windham, W. R., G. H. Poole, B. Park, G. Heitschmidt, S. A. Hawkins, J. P. Albano, T. R. Gottwald, and K. C. Lawrence. 2011. Rapid screening of Huanglongbing-infected citrus leaves by near-infrared reflectance spectroscopy. *Trans. ASABE* 54(6): 2253-2258.